New method to measure the attenuation of hadrons in extensive air showers

W. D. Apel,[1] J. C. Arteaga,[2,*] F. Badea,[1] K. Bekk,[1] M. Bertaina,[3] J. Blümer,[1,2] H. Bozdog,[1] I. M. Brancus,[4] M. Brüggemann,[5] P. Buchholz,[5] E. Cantoni,[3,7] A. Chiavassa,[3] F. Cossavella,[2] K. Daumiller,[1] V. de Souza,[2,†] F. Di Pierro,[3] P. Doll,[1] R. Engel,[1] J. Engler,[1] M. Finger,[1] D. Fuhrmann,[6] P. L. Ghia,[7] H. J. Gils,[1] R. Glasstetter,[6] C. Grupen,[5] A. Haungs,[1] D. Heck,[1] D. Hildebrand,[2,‡] J. R. Hörandel,[2,§] T. Huege,[1] P. G. Isar,[1] K.-H. Kampert,[6] D. Kang,[2] D. Kickelbick,[5] H. O. Klages,[1] Y. Kolotaev,[5] P. Łuczak,[8] H. J. Mathes,[1] H. J. Mayer,[1] J. Milke,[1] B. Mitrica,[4] C. Morello,[7] G. Navarra,[3] S. Nehls,[1] J. Oehlschläger,[1] S. Ostapchenko,[1,‖] S. Over,[5] M. Petcu,[4] T. Pierog,[1] H. Rebel,[1] M. Roth,[1] H. Schieler,[1] F. Schröder,[1] O. Sima,[9] M. Stümpert,[2] G. Toma,[4] G. C. Trinchero,[7] H. Ulrich,[1] J. van Buren,[1] W. Walkowiak,[5] A. Weindl,[1] J. Wochele,[1] M. Wommer,[1] and J. Zabierowski[8]

[1]*Institut für Kernphysik, Forschungszentrum Karlsruhe, 76021 Karlsruhe, Germany*
[2]*Institut für Experimentelle Kernphysik, Universität Karlsruhe, 76021 Karlsruhe, Germany*
[3]*Dipartimento di Fisica Generale dell'Università, 10125 Torino, Italy*
[4]*National Institute of Physics and Nuclear Engineering, 7690 Bucharest, Romania*
[5]*Fachbereich Physik, Universität Siegen, 57068 Siegen, Germany*
[6]*Fachbereich Physik, Universität Wuppertal, 42097 Wuppertal, Germany*
[7]*Istituto di Fisica dello Spazio Interplanetario, INAF, 10133 Torino, Italy*
[8]*Soltan Institute for Nuclear Studies, 90950 Lodz, Poland*
[9]*Department of Physics, University of Bucharest, 76900 Bucharest, Romania*

(Received 27 March 2009; published 23 July 2009)

Extensive air showers are generated through interactions of high-energy cosmic rays impinging the Earth's atmosphere. A new method is described to infer the attenuation of hadrons in air showers. The numbers of electrons and muons, registered with the scintillator array of the KASCADE experiment, are used to estimate the energy of the shower inducing primary particle. A large hadron calorimeter is used to measure the hadronic energy reaching observation level. The ratio of energy reaching ground level to the energy of the primary particle is used to derive an attenuation length of hadrons in air showers. In the energy range from 10^6 to 3×10^7 GeV the attenuation length obtained increases from 170 to 210 $\mathrm{g/cm^2}$. The experimental results are compared to predictions of simulations based on contemporary high-energy interaction models.

DOI: 10.1103/PhysRevD.80.022002 PACS numbers: 96.50.sd, 13.85.Tp, 98.70.Sa

I. INTRODUCTION

Since the earliest days of cosmic-ray investigations it has been realized that these particles provide a unique possibility to study interactions at high energies [1,2]. Even today the energies of cosmic rays exceed the energies achieved in man made accelerators by orders of magnitude. Hence, in the literature many attempts are described to extract properties of high-energy hadronic interactions from air showers induced by cosmic rays in the atmosphere. Among the most interesting quantities is the attenuation length of hadrons (e.g. [3]), in theoretical considerations closely connected to the inelastic cross section.

In the present work, we use the energy absorbed in a material within a certain atmospheric depth X to define an attenuation length. In this new approach we use the number of electrons and muons, registered with a detector array to estimate the energy of the shower inducing primary particle E_0; see (4). The energy reaching the observation level in the form of hadrons $\sum E_H$ is measured with a hadron calorimeter. The fraction of surviving energy in the form of hadrons is defined as

$$R = \frac{\sum E_H}{E_0}. \tag{1}$$

The attenuation length λ_E is then defined as

$$\Sigma E_H = E_0 \exp\left(-\frac{X}{\lambda_E}\right) \tag{2}$$

or

$$R = \exp\left(-\frac{X}{\lambda_E}\right). \tag{3}$$

In the literature different definitions for the attenuation length in air showers are introduced. Frequently, the attenuation length is derived from measurements of the

*Present address: Institute of Physics and Mathematics, Universidad Michoacana, Morelia, Mexico.
†Present address: Universidade de São Paulo, Instituto de Fisica de São Carlos, Brazil.
‡Present address: ETH Zürich, Switzerland.
dorothee.hildebrand@phys.ethz.ch
Corresponding author.
§Present address: Department of Astrophysics, Radboud University Nijmegen, The Netherlands.
‖Present address: Norwegian University, Trondheim, Norway.

electromagnetic shower component, e.g. [4–10]. Investigating single hadrons, the attenuation length is related to the absorption of hadrons in the atmosphere [11]. Pioneering work to derive inelastic cross sections from the measurement of single hadrons has been conducted by Yodh and colleagues [11,12], later followed by the prototype of the KASCADE calorimeter [13].

The new approach presented here is complementary to the different methods described in the literature. In contrast to methods using the electromagnetic shower component, the present work focuses directly on measurements of hadrons to derive an attenuation length for this shower component. The values obtained are not *a priori* comparable to other attenuation lengths since they are based on different definitions. It should be noted that the experimentally obtained attenuation length is affected by statistical fluctuations during the development of the showers. However, in the present work we do not attempt to correct for this effect.

After a description of the experimental situation (Sec. II), the experimental results and comparisons with air shower simulations are described in Sec. III.

II. EXPERIMENTAL SETUP

A. The apparatus

The experiment KASCADE, located on the site of the Forschungszentrum Karlsruhe, 110 m a.s.l., consists of several detector systems. A description of the performance of the experiment can be found elsewhere [14]. A 200×200 m^2 array of 252 detector stations, equipped with scintillation counters, measures the electromagnetic and, below a lead/iron shielding, the muonic components of air showers. In its center, an iron sampling calorimeter of 16×20 m^2 area detects hadronic particles. The calorimeter is equipped with 11 000 warm-liquid ionization chambers arranged in nine layers. Because of its fine segmentation (25×25 cm^2), energy, position, and angle of incidence can be measured for individual hadrons. A detailed description of the calorimeter and its performance can be found in [15]; it has been calibrated with a test beam at the Super Proton Synchrotron at CERN up to 350 GeV particle energy [16].

B. Observables and event selection

The position of the shower axis and the angle of incidence of a cascade are reconstructed by the array detectors. The total numbers of electrons N_e and muons N_μ are determined by integrating their lateral distributions. In the case of muons, the truncated muon number N'_μ is used for experimental reasons. It is the number of muons integrated in the distance range 40–200 m from the shower axis. For a detailed description of the reconstruction algorithms, see [17]. The position of the shower axis is reconstructed with an accuracy better than 2 m and the angle of incidence better than 0.5°.

The hadrons in the calorimeter are reconstructed by a pattern recognition algorithm, optimized to recognize as many hadrons in a shower core as possible. Details can be found in [17]. Hadrons of equal energy can still be separated with a probability of 50% at a distance of 40 cm. The reconstruction efficiency rises from 70% at 50 GeV to nearly 100% at 100 GeV. The energy resolution improves from 30% at 50 GeV to 15% at 10^4 GeV. The hadron number N_h and hadronic energy sum $\sum E_h$ are determined by the sum over all hadrons in a distance up to 10 m from the shower axis. A correction for the missing area beyond the boundaries of the calorimeter is applied. The hadron lateral distributions are relatively steep; the hadronic energy density decreases by about 2 orders of magnitude within the first 10 m from the shower axis [18]. Therefore, it is sufficient to measure hadrons in a relatively narrow range around the shower axis only in order to collect a significant fraction of the total hadron energy. The observable $\sum E_h$ includes also energy of hadrons which could not be reconstructed independently, because they are too close to each other. It shows up in the simulated and experimental data in the same manner.

To be accepted for the present analysis, an air shower has to fulfill several requirements: at least one hadron has been reconstructed in the calorimeter with an energy larger than 50 GeV, the shower axis is located inside the calorimeter, the electromagnetic shower size N_e is larger than 10^4, the truncated muon number N'_μ is larger than 10^3, i.e. the primary energy is greater than about 3×10^5 GeV, and the reconstructed zenith angle is smaller than 30°. From May 1998 to October 2005 312 000 showers have been measured meeting the criteria mentioned.

To avoid corrections for different angles of incidence the following analysis is restricted to showers with zenith angles $\Theta < 18°$. The primary energy E_0 of the shower inducing particle is roughly estimated based on the number of electrons N_e and muons N'_μ registered with the KASCADE scintillator array

$$\log_{10} E_0 \approx 0.19 \log_{10} N_e + 0.79 \log_{10} N'_\mu + 2.33. \quad (4)$$

The average ground pressure during the observation time amounts to 1004 hPa, corresponding to an average atmospheric column density $X_0 = 1023$ g/cm^2. The attenuation is measured at this depth X_0, the average vertical thickness of the atmosphere above the KASCADE experiment.

C. Simulations

The shower simulations were performed using CORSIKA [19]. Hadronic interactions at low energies were modeled using the FLUKA code [20,21]. High-energy interactions were treated with QGSJET 01 ($E > 200$ GeV) [22]. Showers initiated by primary protons as well as helium, carbon, silicon, and iron nuclei have been simulated. The simulations covered the energy range 10^5–10^8 GeV with zenith angles in the interval 0–32°. The energy distribution of the showers followed a power law with a spectral index of −2.0. For the analysis the energy distribution was converted to a power law with an index of −2.7 below and −3.1 above the knee with a rigidity dependent knee position (3×10^6 GeV for protons). The positions of the shower axes are distributed uniformly over an area exceeding the calorimeter surface by 2 m on each side. In order to determine the signals in the individual detectors, all secondary particles at ground level are passed through a detector simulation program using the GEANT package [23]. In this way, the instrumental response is taken into account and the simulated events are analyzed by the same code as the experimental data, an important aspect to avoid biases by pattern recognition and reconstruction algorithms.

III. RESULTS

A. Surviving hadronic energy

The energy of the primary particle is estimated from measurements of the number of electrons and muons in the shower with the scintillator array; see (4). The surviving energy in the form of hadrons ΣE_H is measured with the hadron calorimeter. A fraction R, see (1), of hadronic energy reaching ground level can be inferred as a function of primary energy, as shown in Fig. 1. All error bars represent statistical uncertainties only. Below 10^6 GeV the values are affected by reconstruction efficiencies. In particular, showers induced by heavy elements are less likely to be registered. Therefore, values are shown only for energies exceeding 10^6 GeV. Above 10^7 GeV the flux of the light cosmic-ray component decreases and the composition becomes more and more heavy [24]. Most likely,

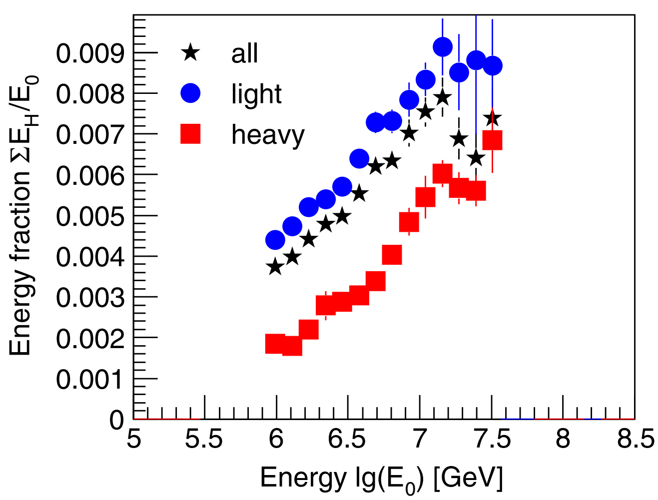

FIG. 1 (color online). Fraction of energy $\Sigma E_H/E_0$ reaching the ground in the form of hadrons as a function of estimated primary energy E_0 for all data and for selections of light and heavy primary particles.

this causes the structures seen in the figure for energies exceeding 10^7 GeV. In the energy range investigated about 0.3 to 0.8% of the primary energy reaches the observation level in the form of hadrons, most of them being pions [13].

In the energy range of interest the elasticity of pions depends only weakly on energy and can be approximated as $\epsilon \approx 0.25$ to 0.3 [25]. With the relation $R = \epsilon^N$, the average number of generations N in the shower can be estimated and it turns out that the registered hadrons (with energies above 50 GeV) have undergone about four to five interactions only. This number is confirmed by full air shower simulations.

The fraction of hadronic energy reaching observation level increases with energy, since the effect of deeper penetrating showers clearly dominates over the small effect caused by the increase of the inelastic cross sections.

The two-dimensional distribution of the number of electrons and muons for the measured showers is depicted in Fig. 2. The stars represent the most probable values of the distribution. Also simulated $N_e - N'_\mu$ distributions have been investigated for primary protons, as well as helium, carbon, silicon, and iron-induced showers. Examples for protons and iron are depicted in Fig. 3. The solid lines represent fits to the most probable values represented by the circles and squares, respectively. It turned out that the slopes of the fits of all elements are about equal. The fitted line for carbon, parametrized as

$$\log_{10}(N_e) = 1.34\log_{10}(N'_\mu) - 0.15 \tag{5}$$

is used in the following to divide the data into a sample induced by "light" and "heavy" primary particles, respectively. It is indicated in Figs. 2 and 3 as dashed lines. In Fig. 3 it can be seen that (5) indeed separates the data set into light and heavy. Almost no iron showers are above the dashed line and only a small fraction of proton-induced showers is below the line. Especially the most probable

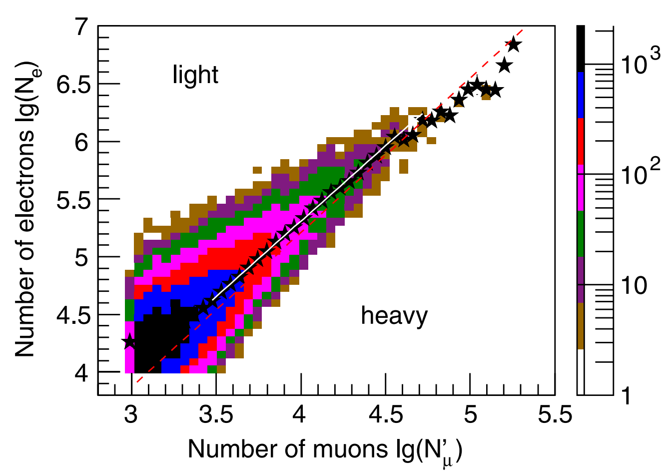

FIG. 2 (color online). The number of electrons and muons for measured showers with zenith angle $\Theta < 18°$. The most probable values of the distribution are indicated by the stars; the solid line represents a fit to this data. The dashed line represents (5).

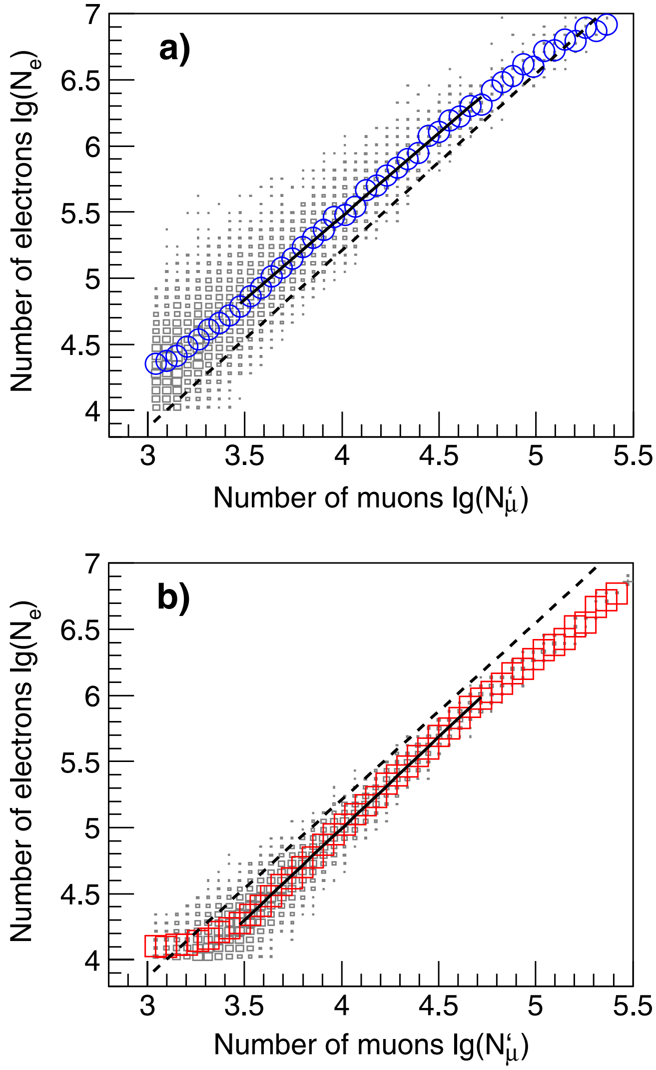

FIG. 3 (color online). The number of electrons vs the number of muons in simulated air showers for primary protons (a) and iron nuclei (b). The solid line indicates a fit to the most probable values (circles and squares, respectively); the dashed lines represent (5).

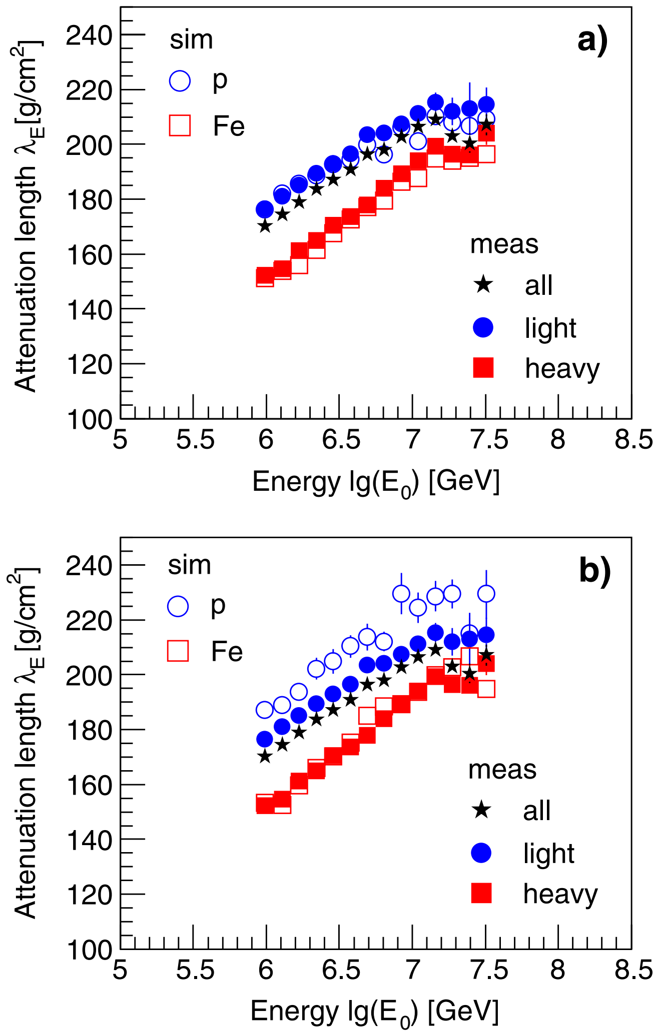

FIG. 4 (color online). Attenuation length λ_E as a function of the estimated primary energy. The light and heavy groups in the measurements are compared to simulations of showers induced by primary protons and iron nuclei using CORSIKA with the hadronic interaction model QGSJET 01 (a) and a modified version with lower cross sections and higher elasticity [(b), model 3a in Ref. [25]].

values for protons and iron-induced showers are clearly above and below the dashed line, respectively. Parametrization (5) almost coincides with the most probable values of the measurements.

Applying the selection criterion (5) to the data, the energy fraction reaching observation level is shown in Fig. 1 as well as for light and heavy primaries. As expected from a simple superposition model, protonlike showers penetrate deeper into the atmosphere and transport more energy to the observation level as compared to ironlike showers.

B. Attenuation length

Using the energy absorbed in the atmosphere at a depth X_0, the attenuation length λ_E has been derived from the measured energy fraction; see (3). The results are presented as a function of the estimated primary energy in Fig. 4(a). Values for the complete data set as well as for the light and heavy selections are shown. The values are compared to results obtained from full air shower simulations for primary protons and iron nuclei using the CORSIKA program with the hadronic interaction generator QGSJET 01. The cuts for a light and a heavy component were applied to the proton and iron simulations in the same way as for the measurements.

The values shown in Fig. 4 have been obtained by applying the same (quality) cuts and reconstruction algorithms to measured and simulated data. Thus, many uncertainties are expected to cancel. For the remaining differences between simulated and measured data a systematic error for the hadronic energy sum ($\sum E_H$) and the total energy (E_0) of 10% each is assumed. With (1) this results in a 14% uncertainty of R. In turn, following (3) yields a systematic error for λ_E of the order of 2%. Therefore, the values shown in Fig. 4 have a systematic uncertainty of the order of 2 to 4 g/cm^2. As discussed above, the structures above an energy of 10^7 GeV are most likely due to the changing composition as a function of energy.

A comparison of the heavy selection with iron-induced showers shows that the heavy selection lies slightly above the simulated values. This makes sense, since the measured data contain a mixture of many elements, most of them being lighter than iron; thus the measurements should be above the iron points. On the other hand, looking at the light selection compared to the proton points from the simulations, one recognizes that at high energies data points are above the simulated values. This cannot be explained by a mixed composition and may be a hint toward a problem in the hadronic interaction model QGSJET 01. A possible explanation is that the attenuation length is too small, i.e. the cross section is too large.

To test this hypothesis simulations have been carried out with a modified version of QGSJET 01, namely, model 3a in Ref. [25]. The inelastic hadronic cross sections have been lowered, e.g. the proton-air cross section at 10^6 GeV is reduced by 5% from 385 to 364 mb and the elasticity has been increased by about 12%. A similar trend to lower cross sections has been found as well by the EAS-TOP experiment, with a value of

$$\sigma_{p\,\mathrm{air}}^{\mathrm{inel}} = 338 \pm 21_{(\mathrm{stat})} \pm 19_{(\mathrm{syst})} - 29_{(\mathrm{syst\,He})}\ \mathrm{mb}$$

at $\sqrt{s} = 2$ TeV ($\approx 2 \times 10^6$ GeV) [10]. At the highest energies the lower proton-air cross section (443 mb at 10^9 GeV) is compatible with recent results from the HiRes experiment

$$\sigma_{p\,\mathrm{air}}^{\mathrm{inel}} = 456 \pm 17_{(\mathrm{stat})} + 39_{(\mathrm{syst})} - 11_{(\mathrm{syst})}\ \mathrm{mb}$$

at 3×10^9 GeV [9]. The lower cross sections have been proposed originally to reduce the discrepancy in the mean logarithmic mass derived from experiments observing shower maximum and investigating particle distributions at ground level [25,26]. Applying the altered version of QGSJET also slightly modifies the number of electrons and muons predicted at ground level. At energies around the knee ($\approx 4 \times 10^6$ GeV) the number of electrons increases by about 5% and the number of muons rises by about 15% [25].

The corresponding results for λ_E are presented in Fig. 4(b). The typical energies of particles in a shower induced by a heavy nuclei are smaller than the typical energies in a proton-induced shower of the same primary energy (superposition model of showers). Thus, the effect of the modifications is stronger for proton-induced showers in Fig. 4(b); see also [25]. In contrast to Fig. 4(a) the simulated points for protons are now above the data points for the light selection. As a result, with the modified version of the interaction model an overall improvement of the situation has been achieved.

It should be pointed out that the experimentally accessible attenuation length λ_E is extremely sensitive to the inelastic hadronic cross sections. A relatively small modification ($\sigma_{p\,\mathrm{air}}$ is changed by 5% only at 10^6 GeV) yields significant changes, as can be inferred from Fig. 4.

In addition, the results have been calculated also as a function of the hadronic energy sum at the observation level. The results for all data, as well as for the light and heavy selections, are presented in Fig. 5(a). Again, a closer

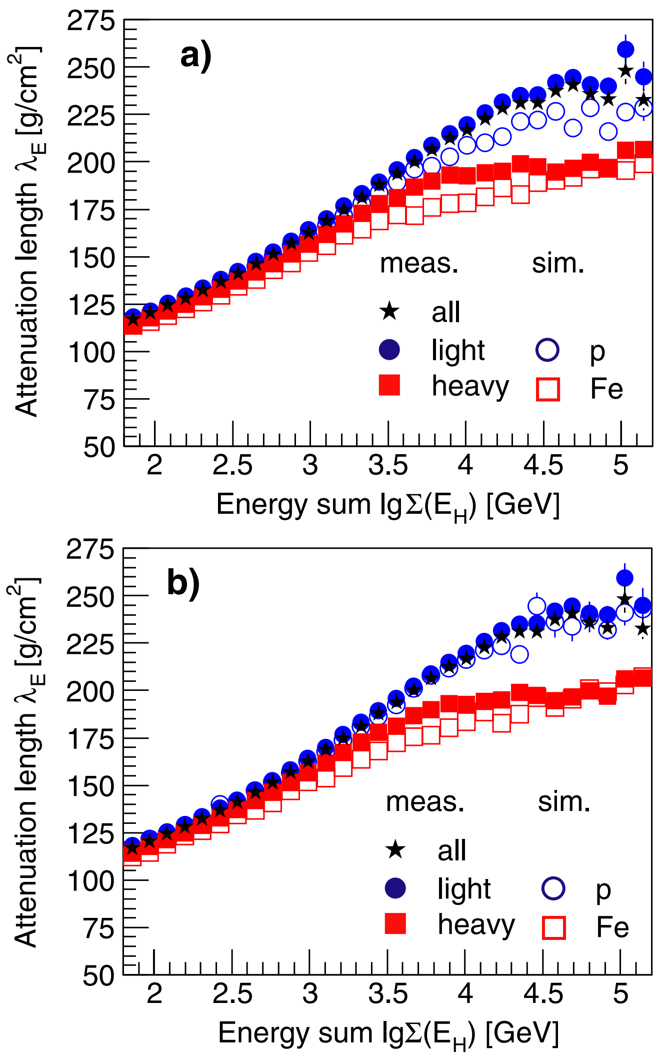

FIG. 5 (color online). Attenuation length λ_E as a function of the measured hadronic energy sum at the observation level. The light and heavy groups in the measurements are compared to simulations for primary protons and iron-induced showers using CORSIKA with the hadronic interaction model QGSJET 01 (a) and a modified version with lower cross sections and higher elasticity [(b), model 3a in Ref. [25]].

inspection yields unreasonable results when the light elements are considered. At high energies even all measured events are above the proton simulations. In agreement with the previous discussion, the issue can be resolved by introducing a modified version of the interaction model, as can be seen in Fig. 5(b). Arranging the data in ΣE_H bins implies an enrichment of light primaries, which explains why all data almost agree with pure proton simulations and the discrepancy between measurements and QGSJET 01 predictions are magnified.

IV. SUMMARY AND CONCLUSIONS

A new method has been developed to derive the attenuation length of hadrons from measurements of high-energy cosmic rays interacting in the Earth's atmosphere. The fraction of the energy of the primary particle reaching ground level in the form of hadrons in air showers has been measured with the KASCADE experiment to increase from about 0.3% at 10^6 GeV to 0.8% at 3×10^7 GeV. An attenuation length based on the absorbed energy has been defined. Corresponding values increase with energy from about 170 to ≈ 210 g/cm^2.

A closer inspection of the attenuation lengths obtained for showers induced by light and heavy elements indicates that the cross sections in the hadronic interaction model QGSJET 01 may be too large and the elasticity may be too small. A modification with altered parameters improves the situation.

As a final remark, it should be pointed out that the attenuation length λ_E is extremely sensitive to inelastic hadronic cross sections. The sensitivity of air shower measurements, in particular, of the hadronic component to properties of hadronic interactions has been demonstrated previously: e.g., the dependence of observable quantities on the transverse momentum in hadronic interactions [27] or on low-energy inelastic cross sections [28]. In a similar way, the data presented and the method introduced in the present article may serve to check and improve further hadronic interaction models.

ACKNOWLEDGMENTS

The authors would like to thank the members of the engineering and technical staff of the KASCADE-Grande Collaboration, who contributed to the success of the experiment. The KASCADE-Grande experiment is supported by the BMBF of Germany, the MIUR and INAF of Italy, the Polish Ministry of Science and Higher Education together with the DAAD (PPP grant for 2009-2010), and the Romanian Ministry of Education and Research (Grant No. CEEX 05-D11-79/2005).

[1] D. Froman and J. Stearns, Rev. Mod. Phys. **10**, 133 (1938).
[2] B. Rossi and K. Greisen, Rev. Mod. Phys. **13**, 240 (1941).
[3] *Encyclopedia of Physics, Volume XLVI/1, Cosmic Rays I*, edited by S. Flügge (Springer Press, Berlin, 1961).
[4] T. Antoni *et al.*, Astropart. Phys. **19**, 703 (2003).
[5] T. Hara *et al.*, Phys. Rev. Lett. **50**, 2058 (1983).
[6] M. Honda *et al.*, Phys. Rev. Lett. **70**, 525 (1993).
[7] M. Aglietta *et al.*, Nucl. Phys. B, Proc. Suppl. **75A**, 222 (1999).
[8] R. Baltrusaitis *et al.*, Phys. Rev. Lett. **52**, 1380 (1984).
[9] K. Belov *et al.*, Nucl. Phys. B, Proc. Suppl. **151**, 197 (2006).
[10] M. Aglietta *et al.*, Phys. Rev. D **79**, 032004 (2009).
[11] G. Yodh *et al.*, Phys. Rev. Lett. **28**, 1005 (1972).
[12] R. Ellsworth *et al.*, Phys. Rev. D **26**, 336 (1982).
[13] H. Mielke *et al.*, J. Phys. G **20**, 637 (1994).
[14] T. Antoni *et al.*, Nucl. Instrum. Methods Phys. Res., Sect. A **513**, 490 (2003).
[15] J. Engler *et al.*, Nucl. Instrum. Methods Phys. Res., Sect. A **427**, 528 (1999).
[16] S. Plewnia *et al.*, Nucl. Instrum. Methods Phys. Res., Sect. A **566**, 422 (2006).
[17] T. Antoni *et al.*, Astropart. Phys. **14**, 245 (2001).
[18] T. Antoni *et al.*, J. Phys. G **25**, 2161 (1999).
[19] D. Heck *et al.*, Forschungszentrum Karlsruhe Report No. FZKA 6019, 1998.
[20] A. Fasso *et al.*, CERN Report No. CERN-2005-10, INFN Report No. INFN/TC-05/11, SLAC Report No. SLAC-R-773, 2005.
[21] A. Fasso *et al.*, arXiv:hep-ph/0306267.
[22] N. Kalmykov *et al.*, Nucl. Phys. B, Proc. Suppl. **52B**, 17 (1997).
[23] *Geant 3.21 Detector Description and Simulation Tool*, CERN Program Library Long Writeup W5013, CERN, 1993.
[24] H. Ulrich *et al.*, Astropart. Phys. **24**, 1 (2005).
[25] J. Hörandel, J. Phys. G **29**, 2439 (2003).
[26] J. Hörandel, Nucl. Phys. B, Proc. Suppl. **151**, 75 (2006).
[27] T. Antoni *et al.*, Phys. Rev. D **71**, 072002 (2005).
[28] W. Apel *et al.*, J. Phys. G **36**, 035201 (2009).